PART Ⅲ

Part III Conclusion

Chapter 1 Conclusion

1.1 Geophysical Prospecting

1.1.1 Applicability of Geophysical Prospecting Methods

Geophysical prospecting, using gravity, IP and magnetic methods, was carried out in the El Akhouat-Argoub Adama and Bou Khil prospects during the 1st Year Campaign. Laboratory testing of rock samples was also conducted to specify physical properties of various types of rocks for interpreting geophysical signatures. The resultant geophysical anomalies and indications were explored by drilling during the 2nd Year Campaign for verification their causes. Based on the results of all these works, the prospecting methods employed in the current exploration project are assessed for their applicability to the mineral exploration in the Project Area as summarized below.

(1) Chargeability is effective to outline mineralized zones, because high chargeability has been indicated in the mineralized rock samples by the laboratory testing and in association with the known ore deposits or the mineralized zones intersected by the drilling.

(2) Intensity of chargeability can be correlated to intensity of mineralization. Because high chargeability exceeding 20 mV/V is indicated in the vicinity of the drill holes that intersected the mineralized zones, while chargeability is moderate at around 10 mV/V where mineralization is weak and consists mainly of pyrite.

(3) Anomalously low resistivity of 1 Ωm or less is indicated in the sandstone with high pore pressure intersected by the drill holes in the Bou Khil prospect. Well and surface water indicates high conductivity of 1 mS/cm or higher according to the result of conductivity measurement. Therefore, such anomalously low resistivity suggests sandstone with high pore pressure being filled with highly conductive water. Sandstone with high pore pressure will potentially make difficult ground for drilling or underground excavation.

(4) Transition zones, accompanying mineralization, are located between the Triassic and Cretaceous or Tertiary systems, in either flanks of high gravity anomalies forming anticlinal structures, in the vicinity of steep slopes of residual gravity structures or in association with discontinuous zones of

resistivity.

(5) It will be possible to locate subsurface Triassic diapirs associated with transition zones by the gravity cross-section analysis combined with the resistivity cross-section analysis of IP measurements.

The above assessment leads to the conclusion that the geophysical prospecting will delineate exploration targets as high chargeability anomalies associated with transition zones in the vicinity of diapirs where no resistivity anomaly of 1 Ωm or less is detected.

1.1.2 Bazina Kebira Prospect

No chargeability anomaly exceeding 10 mV/V has been detected in Bazina Kebira prospect. Therefore, no exploration target that can be compared to those in the Bou Khil and the El Akhouat-Argoub Adama in terms of intensity of chargeability has been delineated. However, the four mineral indications except the Bazina Kebira show relatively high chargeability compared to that in other part of the prospect. Chargeability exceeding 5 mV/V at an elevation of 300m is observed only in two localities, in the vicinities of the H'Zamel indication and the Koudiat Soda deposit, respectively in the southwestern and the northeastern parts of the Project Area.

The chargeability anomaly associated with the H'Zamel indication is located in the Cretaceous system close to the contact to the Triassic system that indicates a fair agreement with the position of the resistivity discontinuity. This location of the chargeability anomaly corresponds to the part of the gravity anomaly(gravity high) jutting out southwestwards towards the El Aroussa plain from the Djebel Ech Chied Hills. This feature relative to the gravity structure is resemble to that of the chargeability anomaly associated with the old workings of Bou Khil Mine. In addition, this chargeability anomaly is located in a part of a local high of residual resistivity suggesting a transition zone. The chargeability anomaly is, however, bounded by low resistivity outlined by the 1 Ωm contour, which should be taken into account in planning a drilling exploration program for hole locations, directions and inclinations.

The chargeability anomaly associated with the Koudiat Soda deposit is located along the contact of the Triassic system to the Cretaceous and Tertiary systems. The associated residual gravity structures and resistivity distribution are very complex. The laboratory test of the ore samples collected from the Koudiat Soda deposit has indicated the maximum of 100 mV/V, which suggests that the anomaly may have been caused by mineralization. The anomaly is located along the baseline, C0, extending from the intersection of the baseline and the measuring line, C15, on the northeastern slope. Though being located in the high resistivity zone, the anomaly is surrounded by low resistivity anomalies outlined by the 1 Ωm contour, which should be taken into account in planning a drilling exploration program for hole locations, directions and inclinations.

1.1.3 Siliana Prospect

Chargeability of Siriana prospect is very low, even lower than in Bazina Kebira prospect, without yielding any measurements exceeding 5 mV/V. No chargeability anomaly has been detected in association with the two mineral indications in the prospect, which suggests that the mineralization is very much limited in its extent for both indications, if any. Weak chargeability anomalies outlined by the 4 mV/V contour at an elevation of 150m are located only at the northeastern end of the measuring line A6 and at the intersection of the baseline A0 and the measuring line A7 with limited extensions. These anomaly are situated in zones of high residual gravity and high resistivity in the Cretaceous system and associated with calcite veins carrying minor galena at the latter location. It may be implied, therefore, that the anomalies may be related to mineralization regardless of its intensity and extension. A subsurface chargeability anomaly is also outlined by the 4 mV/V contour at depth between the stations 70 and 80 of the measuring line A5. This anomaly is associated with a high resistivity anomaly surrounded by low resistivity anomalies and is situated in close proximity to a subsurface diapir interpreted from the gravity cross-section analysis. This implies that the anomaly may be an indication of a transition zone.

1.1.4 El Akhouat-Argoub Adama Prospect

In El Akhouat-Argoub Adama prospect where mineralized zones were intersected by drilling in the 2nd Year Campaign, a chargeability anomaly outlined by the 10 mV/V contour extends in an appreciable area centering the hole location of MJTK-L2, in the vicinity of which chargeability exceeds 20 mV/V. The geophysical prospecting of the 2nd Year Campaign was carried out to explore the southwestern extension of this chargeability anomaly. The result indicates that the anomaly continues southwestward for about 500 m only to the survey line L2 with its high chargeability zone being limited along the survey line L3. A lateral fault that runs between the two survey lines may bound the southwestern extension. It is necessary to carry out an IP survey along the line L6 in order to northwesterly track the high chargeability zone exceeding 20 mV/V. In the 1st Year IP survey, high chargeability better than 20 mV/V was recorded at the northwestern end of the line L6, as well as along the line L3. Therefore, the line L6 will have to be extended northwesterly for 500m in order to achieve this purpose.

1.2 Drilling Investigation

1.2.1 Bou Khil Prospect

(1) The hole MJTK-B1 that aimed at verification of the IP anomaly and exploration of the extension of the known deposit intersected the celestite mineralization with the width of 18m and the average grade of 17.19 % $SrSO_4$. The grade of marketable celestite should be 88 % $SrSO_4$ or higher. Therefore, exploitation of the celestite mineralization is regarded as economically inviable.

(2) The hole MJTK-B2 that aimed at verification of the IP anomaly failed to intersect any mineralization. Pb-Zn mineralization in the Tertiary system had been expected since the IP anomaly was associated with Tertiary formations. The cause of the IP anomaly is, however, proved to be pyrite in sandstone.

1.2.2 El Akhouat-Argoub Adama Prospect

(1) The hole MJTK-L1 aimed at verification of the IP anomaly and exploration of possible mineralization in the Cretaceous formations distributing around a diapir. This hole intersected only weak Pb-Zn mineralization. It is interpreted that the mineralization is weak because the Cretaceous formations distributing around a diapir belong to Aptian and are different from those hosting the major ore deposits in their stratigraphic positions. The cause of the IP anomaly is proved to be abundant pyrite contained in the formations comprising Aptian marl.

(2) The hole MJTK-L2 was drilled to verify the new mineralization located in the course of the 1st Year Campaign. This hole intersected three mineralized zones with the widths of 16.0m (the average grade of 4.27 % Pb+Zn), of 11.8m (the average grade of 6.30 % Pb+Zn) and of 32.0m (the average grade of 4.14 % Pb+Zn) in the host rocks of Cretaceous carbonates in the interval between 225.50 and 382.90m. In addition, these mineralized zones include three 1m-sections of carbonate-hosted ores indicating 0.7 % Pb and 20.0 % Zn from 237.50 to 238.50m, 1.92 % Pb and 36.0 % Zn from 275.60 to 276.60m, and 3.45 % Pb and 16.0 % Zn from 379.90 to 380.90m. It is the most essential subject for the current exploration program to explore the continuities and the extensions of these mineralized zones.

(3) The hole MJTK-L3 was drilled to explore mineralization in the Cretaceous system and to verify the IP anomaly detected by the 1st Year IP survey and the subsurface diapir interpreted from the result of the gravity survey. This hole intersected pyrite-calcite veinlets/networks carrying minor sphalerite and galena as well as celestite-calcite or pyrite-calcite veinlets/networks accompanying minor sphalerite

in association with brecciated zones. However, no mineralization has been intersected with any significant concentration. The cause of the IP anomaly can be correlated to black compact dolomite accompanying a significant amount of pyrite within a diapir body. This diapir, in its position, corresponds to the interpreted subsurface diapir according to the result of the gravity survey.

(4) The hole MJTK-L4 was drilled to explore the southwestern extension of the mineralization intersected by the hole MJTK-L2. This hole intersected mineralization that consists of pyrite-calcite veinlets/networks carrying minor galena and sphalerite. However, the mineralization indicates no significant concentrations in either lead or zinc. The cause of the IP anomaly can be attributed to marl accompanying abundant pyrite.

Chapter 2 Recommendations for the Third Year Campaign

The geophysical prospecting carried out in the 2nd Year Campaign failed to indicate any significant chargeability anomaly either in the Bazina Kebira or in the Siriana prospect. No further geophysical exploration will be recommended for the two prospects. However, it may be worthwhile to track the anomalous chargeability detected at the northeastern end of the line A6 in the eastern Siriana prospect northeastwards to the Assioud mineral indication.

In the El Akhouat-Argoub Adama prospect, it will be necessary to apply the gravity and the IP methods to the lines L4, L9 and L10 that have been prospected only by the magnetic method. It will be also recommended to drill-explore the chargeability anomaly exceeding 20 mV/V, located along the line L6, and to extend the geophysical prospecting northwestward along this line.

Among the mineral indications in the Krib-Mejez el Bab Area, three indications, namely Jebel Bou Mouss, Kef Lasfer and Oued Jebes where no geophysical prospecting has been made will be worthwhile for geophysical prospecting. A new regional exploration scheme would be recommended for an area including these mineral indications.

REFERRENCES

REFERENCES

物理探査学会(1999) 第5章 電気探査, 物理探査ハンドブック, p. 239-296.

————(1999) 第8章 重力探査, 物理探査ハンドブック, p. 433-468.

千葉昭彦・熊田政弘(1994) 花崗岩及び凝灰岩試料の比抵抗測定－間隙水の比抵抗が岩石比抵抗に及ぼす影響について－. 物理探査, Vol. 47, p. 161-172.

Chikhaoui, M., Hatira, N., Khalfaoui, A. et Hamouda, A. (1993) Etude geologique et geochimique du prospect de L'oued Jebs, secteur de Mejez El Bab resultants et proposition de sondages: Association ONM-MG Centre Zitoua, Le Kef.

Coggon, J. H. (1971) Electromagnetic and electrical modeling by the finite element method. Geophysics, Vol. 36, No. 1, p. 132-155.

Cooperation ONM-BRGM(1982-1985) Projet zone des domes, Inventaire gitologique, Feuille au 1/50.000 Gafour: Office National Des Mines, Bureau de Recherches Geologiques et Minieres.

————(1982-1985) Projet zone des domes, Inventaire gitologique, Feuille au 1/50.000 Medjez El Bab: Office National Des Mines, Bureau de Recherches Geologiques et Minieres.

————(1982-1985) Projet zone des domes, Inventaire gitologique, Feuille au 1/50.000 Teboursouk: Office National Des Mines, Bureau de Recherches Geologiques et Minieres.

Cox, D. P. and Singer, D. A., eds. (1986) Mineral deposit model. U.S. Geol. Surv. Buii., 1693, 379p.

Dali, F. (1995) Notice explicative de la carte géologique de la Tunisie à 1/50.000, Gafour, Feuille n°40: Republique Tunisienne Ministere de L'industrie, Office National des Mines, Direction de la Géologie.

Dey, A. and Morison, H. F. (1979) Resistivity modeling for arbitarily shaped two-dimensional structures. Geophysical Prospecting, Vol. 27, p. 106-136.

Fakraoui, M., Ghanmi, M. et Hatira, N. (1998) Notice explicative de la carte géologique de la Tunisie à 1/50.000, Nebeur, Feuille n°39: Republique Tunisienne, Ministere de L'industrie, Office National des Mines, Service Géologique de Tunisie.

Hammami, M. (1993) Mise au point sur les travaux tactiques realizes sur le flanc est du Jebel Ech Cheid: Office National des Mines, Direction de la Recherche Miniere, Division Inventaire.

————(1993) Travaux de recherche effectues sur le flanc est du Jebel El Akhouat: Office National Des Mines, Direction de la Recherche Miniere, Division Inventaire.

————(1996) Donnees geologiques, gitologiques, geochimiques de l'alignement J. Ech Cheid-J. El Mourra(Teboursouk-Mejez El Bab). Volume 3:D-Donnees gitologiques: Office National Des Mines, Division Inventaires, Projet: Recherche D'anomalies.

Hatira N., Perthuisot V. and Rouvier H. (1990) Les minéraux à Cu, Sb, Ag, Hg des minerais à Pb-Zn de Sakiet Koucha(diapir de Sakiet Sidi Youssef, Tunisie Septentrionale). Mineral Depos, Vol. 25, p. 112-117.

Jean-Claude, G. (1999) Expertise des leves gravimetriques CG-01 et CG-02. (Zone des Domes Tunisie): Office National des Mines de Tunisie.

加藤元彦(1987) 2次元フィルタの理論と重力・磁力分布の解析. ラテイス社, 262p.

Pelton, W.H., Rijo, L. and Swift, C.M.(1978) Inversion of two-dimensional resistivity and induced-polarization data. Geophysics, Vol.43, No.4, p.788-803.

Perthuisot, V.(1979) Carte géologique de la Tunisie, Echelle:1/50.000, Feuille n°33 Teboursouk, Notice explicative: Republique Tunisienne, Ministere de L'industrie des Mines et de L'energie, Direction des Mines et de la Géologie, Sous Direction de la Géologie.

Perthuisot V., Bouzenoune A., Hatira N., Henry B., Laatar E., Mansouri A., Rouvier H., Smati A. et Thibieroz J.(1999) Les diapirs du Maghreb orien: part des déformations alpines et des structures initiales crétacées et éocènes dans les formes actuelles. Bull.Soc.géol.France, t.170, no 1, p.57-65.

Republique Tunisienne, Ministere de L'economie Nationale, Office National des Mines, Departement de la Géologie, Service Géologique National(1985) Carte Géologique de la Tunisie, Echelle 1:500.000

Rouvier, H., Perthuisot, V. and Mansouri, A.(1985) Pb-Zn deposits and salt-bearing diapirs in southern Europe and north Africa. Economic Geology, vol.80, p.666-687.

Sasaki, Y.(1992) Resolution of resistivity tomography inferred from numelical simulation. Geophysical Prospecting, Vol.27, p.106-136.

(財) 資源・環境観測解析センター(1996) 新編リモートセンシング用語辞典

(財) 資源観測解析センター(1989) 資源探査のためのリモートセンシング実用シリーズ別冊用語辞典

————(1992) 資源探査のためのリモートセンシング実用シリーズ5合成開口レーダー (SAR)

Stranik, Z., Biely, A. et Salaj, J.(1994) Notice explicative de la carte géologique de la Tunisie à 1/50.000, Oued Zarga, Feuille n°26: Republique Tunisienne, Ministere de L'industrie, Office National Des Mines, Direction de la Géologie.

Zonge Engineering(1994) GDP-32 Instruction Manual 5-5.28.

APPENDIXES

Appendix 1 Result of Microscopic Observation for Rock Thin Sections

No.	Drill-hole	Depth (m)	Rock Name	Minerals											
				Primary							Secondary and Alteration				
				Qz	Dol	Pl	Bio	Mus	Cal	Oq	Qz	Ch	Cal	Oq	Others
1	MJTK-B1	72.30	Metamorphosed Dolomite	△	◎			?	○	○	+		△	+	wollastonite
2	MJTK-L2	19.30	Dolomite		◎				◎		+				layered structure
3	MJTK-L2	33.00	Dolomite		◎				○						layered structure
4	MJTK-L2	50.00	Dolomite		◎				○						
5	MJTK-L2	66.00	Dolomite		◎				○				△		
6	MJTK-L2	85.00	Dolomite		◎				○				○	△	
7	MJTK-L2	138.20	Dolomite		◎		?		○	+		?			
8	MJTK-L2	275.00	Limestone		△				◎				○	+	
9	MJTK-L2	280.70	Dolomite/Sandstone	○	◎	○	?	?	○	+		?	○		layered structure
10	MJTK-L2	356.40	Metamorphosed Dolomite	+	◎				◎	○			○		wollastonite

Appendix 2 Result of Microscopic Observation for Polished Sections

No.	Drill-hole	Depth (m)	Ore Type	Ore Minerals						
				Galena	Sphalerite	Marcasite	Pyrite	Goethite	Cerestite	Texture
1	MJTK-B1	49.50	Celestite ore			+			◎	framboidal
2	MJTK-B1	63.00	Celestite ore		+	△	+		○	framboidal
3	MJTK-L2	277.00	Veinlet		◎	◎				framboidal
4	MJTK-L2	297.60	Banded	◎	○	△	+			
5	MJTK-L2	298.60	Network veins	+	◎	○	+			
6	MJTK-L2	299.60	Brecciated	△	○	◎				poikilitic
7	MJTK-L2	300.60	Brecciated	○	◎	△				colloform
8	MJTK-L2	301.60	Banded		◎	○	+	+		colloform
9	MJTK-L2	380.60	Brecciated	○	○	△	△			
10	Koudiet Souda		Veinlet	○	◎		△			framboidal

◎: abundant(>50%), ○: moderate(50-20%), △: a few(20-5%), +: rare(<5%),

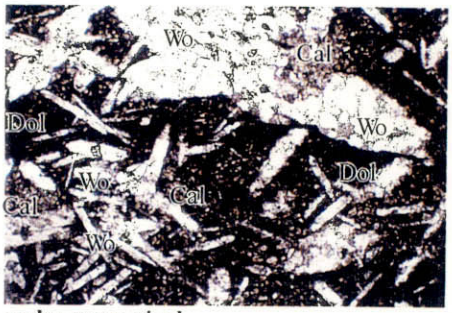

under open nicol

under crossed nicols

Drill-hole:
MJTK-B1
Depth:
72.30m

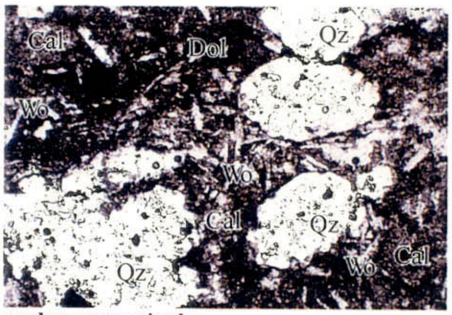

under open nicol

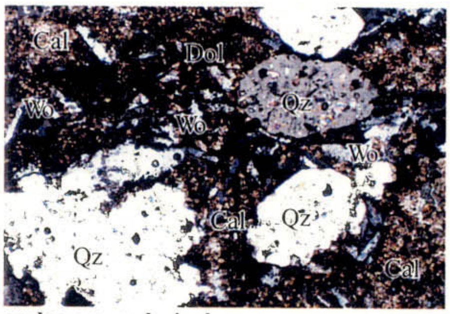

under crossed nicols

0 0.5 1.0mm
Scale of microphoto

Metamorphosed Dolomite

This rock shows very dark brown and partly white in color. Constituent minerals are dolomite, calcite (~ 0.2 mm), quartz (~ 0.8 mm), opaque minerals and lath-shaped wollastonite (~ 1 mm). The wollastonite crystals are formed by metamorphism. Secondary calcite vein is developed.

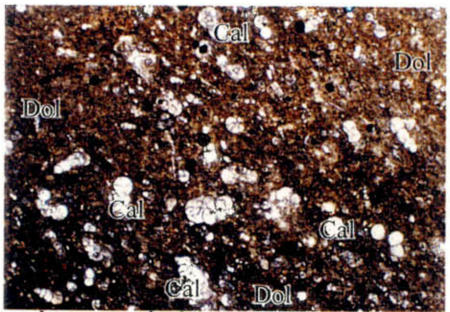

under open nicol

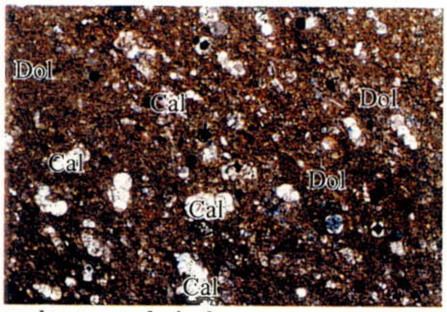

under crossed nicols

Drill-hole:
MJTK-L2
Depth:
19.30m

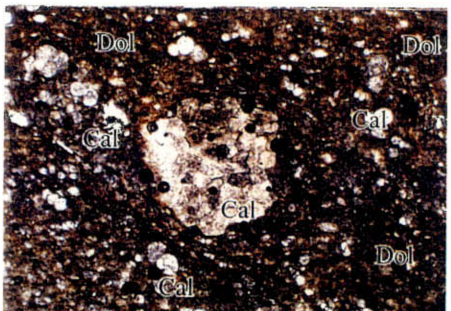

under open nicol

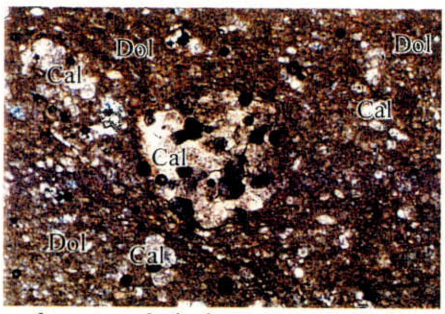

under crossed nicols

0 0.5 1.0mm
Scale of microphoto

Dolomite

This rock shows brownish gray in color and layered structure with pore-space. Constitute minerals are dolomite, calcite (~ 0.1 mm) and quartz (~ 0.2 mm). Most fossils are spherical shape and partly lath-shaped. The pore-space is filled by secondary quartz.

Appendix 3 Microphotographs of thin sections (1)

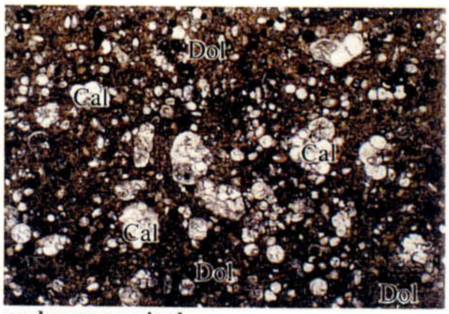

under open nicol

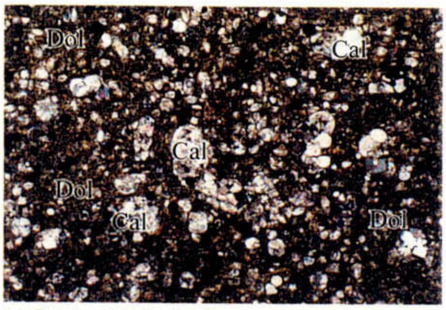

under crossed nicols

Drill-hole:
MJTK-L2
Depth:
33.00m

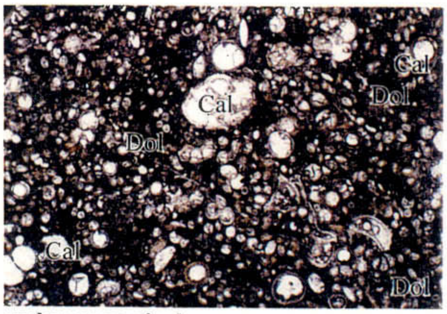

under open nicol

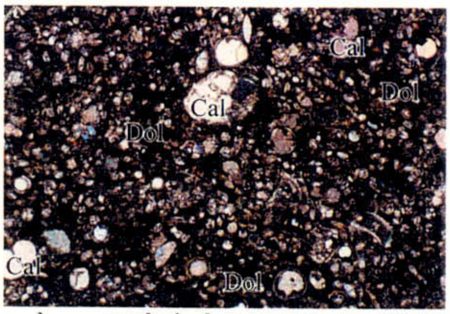

under crossed nicols

0 0.5 1.0mm

Scale of microphoto

Dolomite

This rock shows dark gray. The rock is similar to the sample from 50.00m, whereas many microfossils are recognized in this rock than the sample. Constituent minerals are dolomite and calcite (~ 0.2 mm). Most fossils are spherical shape and partly lath-shaped. Calcite vein is recognized.

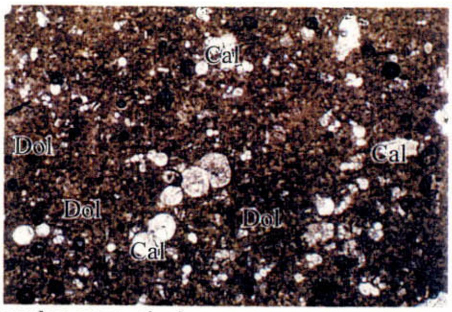

under open nicol

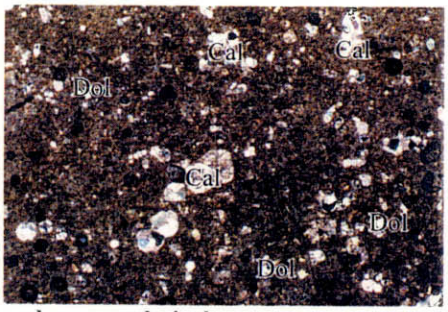

under crossed nicols

Drill-hole:
MJTK-L2
Depth:
50.00m

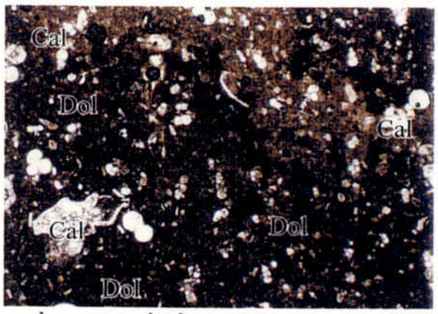

under open nicol

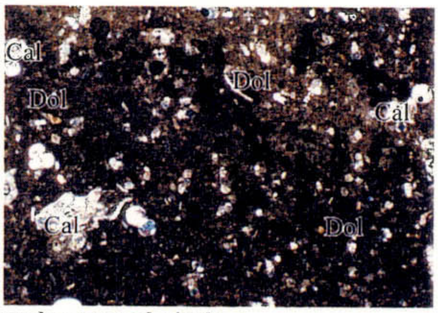

under crossed nicols

0 0.5 1.0mm

Scale of microphoto

Dolomite

This rock shows light gray in color. Constituent minerals are dolomite and calcite (~ 0.2 mm). Most fossils are spherical shape and partly lath-shaped. Calcite vein is recognized.

Appendix 3 Microphotographs of thin sections (2)

Drill-hole:
MJTK-L2
Depth:
66.00m

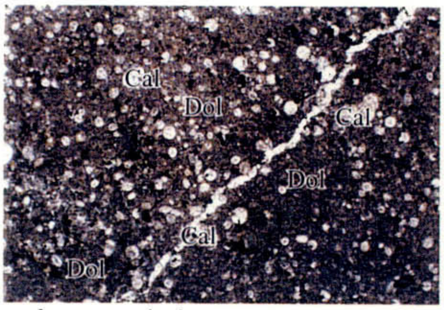

under open nicol

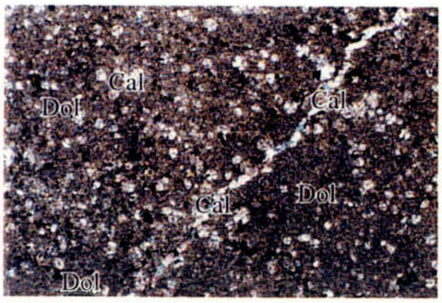

under crossed nicols

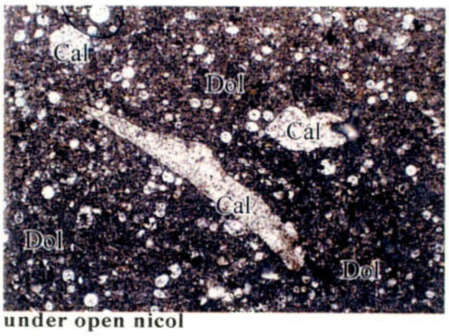

under open nicol

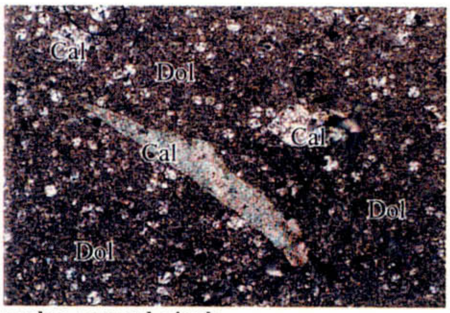

under crossed nicols

0 0.5 1.0mm

Scale of microphoto

Dolomite

This rock shows light gray in color and consists of dolomite and calcite. Most fossils (~ 0.2 mm) are spherical shape and partly lath-shaped. Secondary calcite veins are developed. This rock has no layered structures.

Drill-hole:
MJTK-L2
Depth:
85.00m

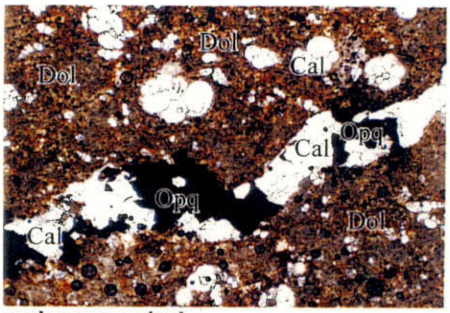

under open nicol

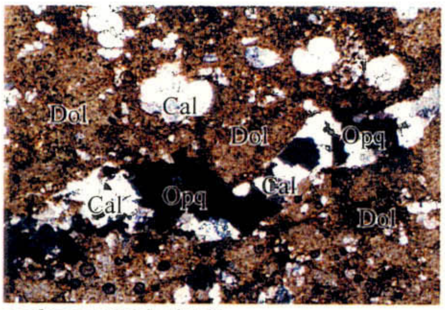

under crossed nicols

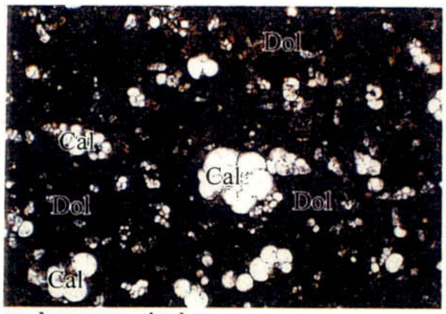

under open nicol

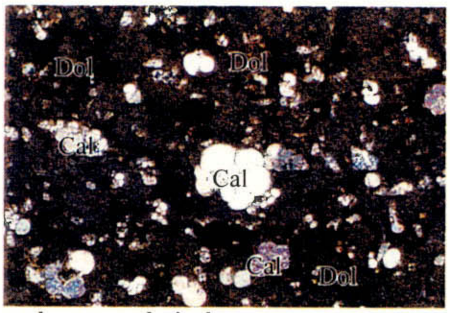

under crossed nicols

0 0.5 1.0mm

Scale of microphoto

Dolomite

This rock shows light gray and is more fine-grained than samples from 19.30m and 66.00m. The rock mainly consists of dolomite with calcite and opaque minerals (~ 0.1 mm). Most fossils are spherical shape. Opaque minerals are grown up along secondary calcite vein.

Appendix 3 Microphotographs of thin sections (3)

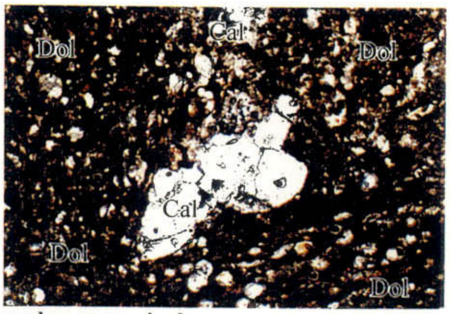

under open nicol

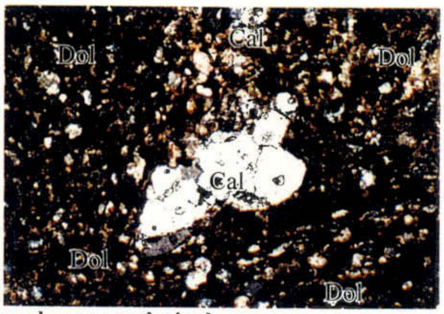

under crossed nicols

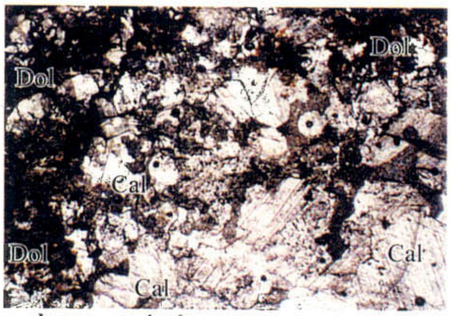

under open nicol

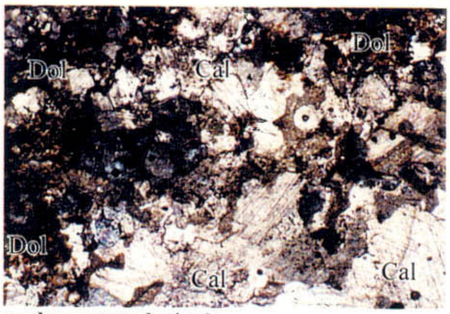

under crossed nicols

Drill-hole:
MJTK-L2
Depth:
138.20m

0 0.5 1.0mm

Scale of microphoto

Dolomite

This rock shows very dark brown in color and consists of dolomite and calcite. Most fossils (~ 0.2 mm) are spherical shape and partly lath-shaped. Secondary calcite veins are recognized.

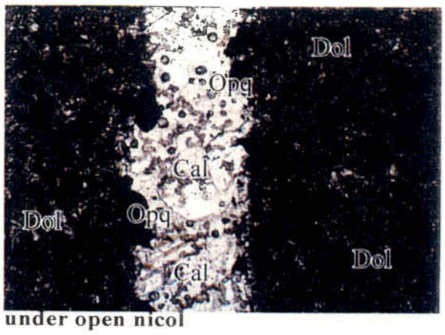

under open nicol

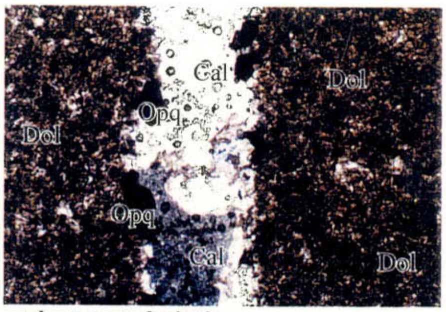

under crossed nicols

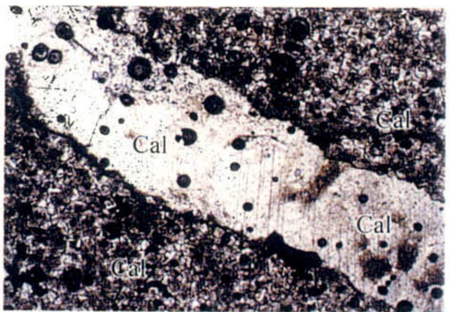

under open nicol

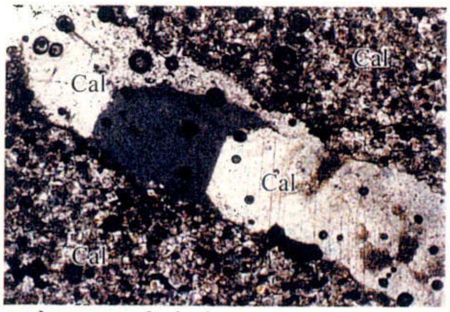

under crossed nicols

Drill-hole:
MJTK-L2
Depth:
275.00m

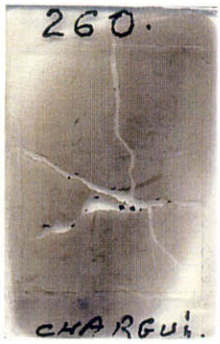

0 0.5 1.0mm

Scale of microphoto

Limestone

This rock shows light gray. The rock consists of calcite, dolomite (~ 0.2 mm) and opaque minerals. Calcite vein including pyrite crystals (~ 0.5 mm) is developed. Microfossils are not recognized.

Appendix 3 Microphotographs of thin sections (4)

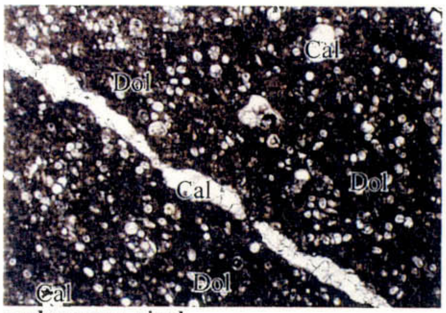

under open nicol

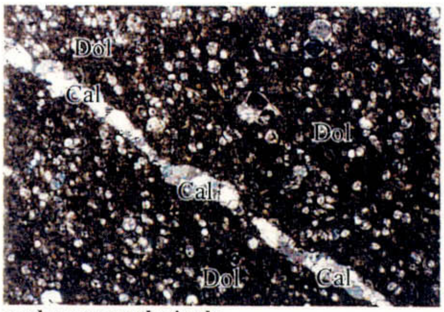

under crossed nicols

Drill-hole:
MJTK-L2
Depth:
280.70m

0 0.5 1.0mm
Scale of microphoto

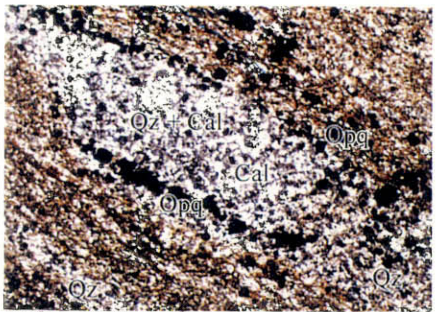

under open nicol

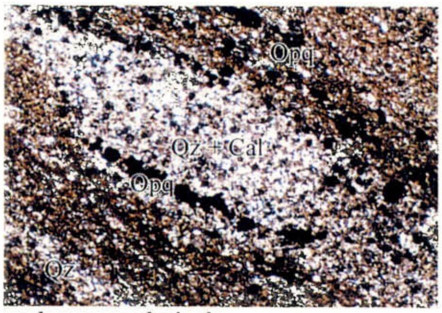

under crossed nicols

Dolomite/Sandstone

This rock is divided in two parts. One part is same as the sample from 85.00m and other part is fine-grained sandstone. The sandstone is consists of quartz, feldspars (~ 0.2 mm) and calcite (~ 0.2 mm), and has layered structures. Secondary calcite veins with opaque minerals are developed.

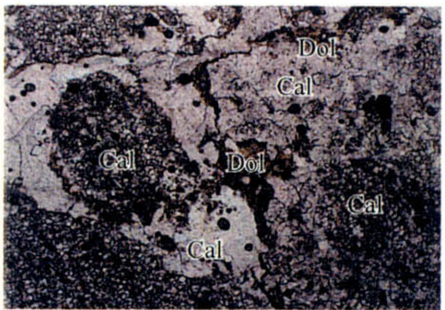

under open nicol

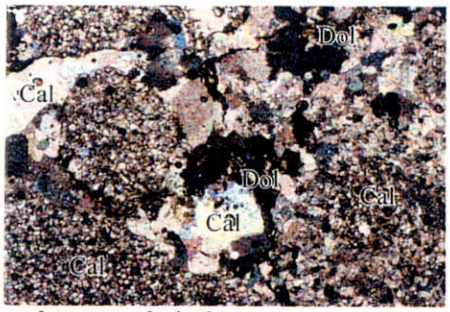

under crossed nicols

Drill-hole:
MJTK-L2
Depth:
356.40m

0 0.5 1.0mm
Scale of microphoto

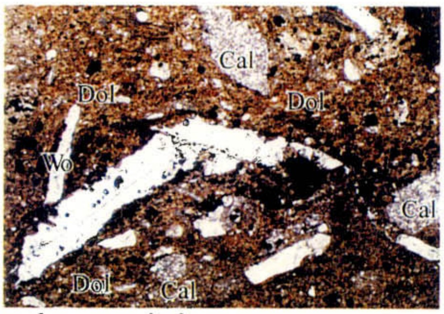

under open nicol

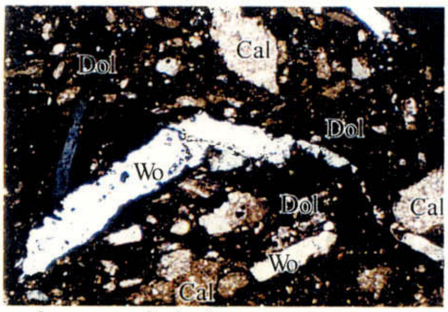

under crossed nicols

Metamorphosed Dolomite

This rock shows dark gray and includes some limestone blocks. Constituent minerals are dolomite, calcite, opaque minerals (~ 0.2 mm) and lath-shaped wollastonite (~ 0.5 mm). The wollastonite crystals are formed by metamorphism. Secondary calcite and opaque mineral veins are developed.

Appendix 3 Microphotographs of thin sections (5)

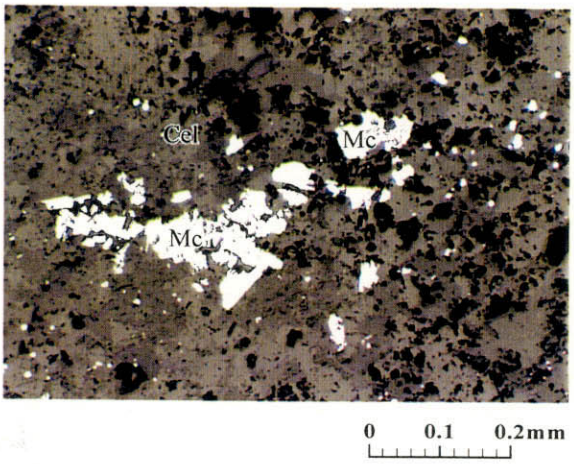

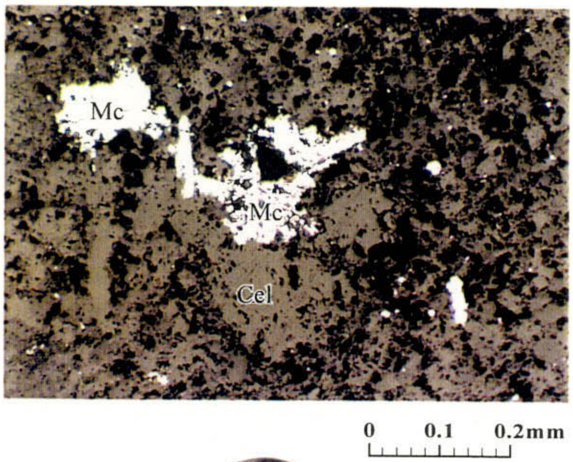

Drill-hole: **Depth:** **Ore type:**

MJTK-B1 49.50m Celestite Ore

The sample contains celestite with the volume ratio of about 60%. The sample is hydrothermally disseminated by marcasite. Under microscope, the color of celestite is greenish grey, and the reflectance is lower than quartz. Celestite occurs at the grain boundary of all kinds of minerals, suggesting minerals at the last stage. Celestite occurs as aggregates of tabular or fabric crystals up to 0.05mm in size. Many grains shows euhedral to subhedral shape. The size of marcasite is up to 0.2mm. Many grains shows euhedral to subhedral shape, and occasionally fine marcasites are gathered together to form framboidal texture. Other opaque mineral is not observed.

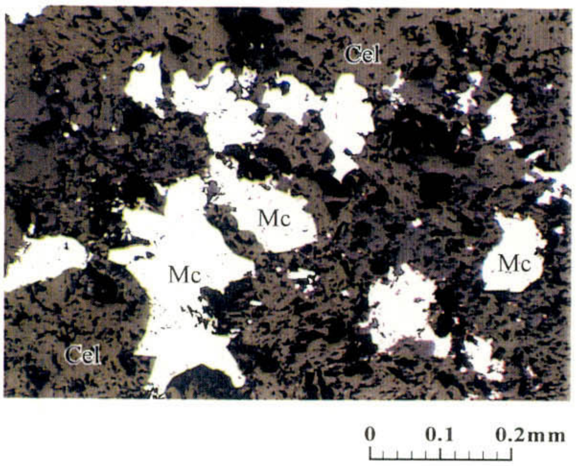

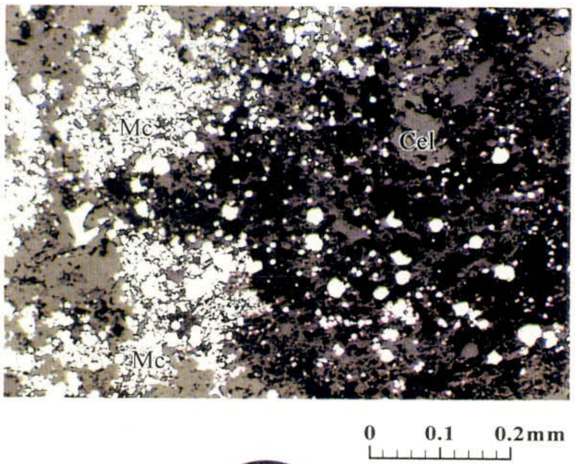

Drill-hole: **Depth:** **Ore type:**

MJTK-B1 63.00m Celestite Ore

The sample is a celestite ore. The volume percentage of celestite is about 30%, and occurs as veins or bands in hydrothermally altered rocks, coexisting with sulfide minerals and silicate minerals. Celestite occurs as tabular crystals with the size up to 0.01 x 0.05 mm. The sulfide minerals are marcasite (almost 100 vol.% among opaque minerals), pyrite (minor) and sphalerite (minor). Marcasite shows framboidal texture whose size is up to 0.05mm. Some grains shows euhedral shape. Pyrite is found in the framboidal marcasite as small subhedral crystals (0.02 mm). Sphalerite occurs as subhedral crystals, coexisting with marcasite. The size is about 0.05 mm.

Appendix 4 Microphotographs of ore polishes (1)

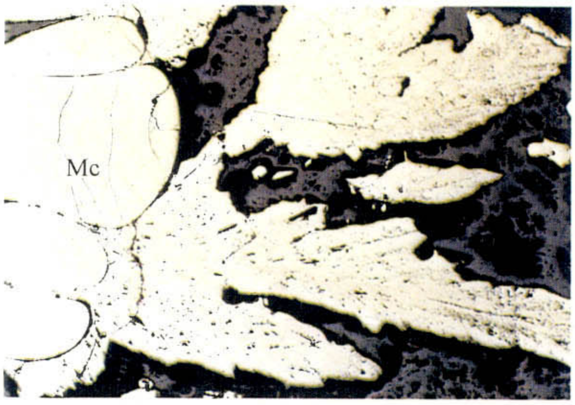

0 0.2 0.4mm

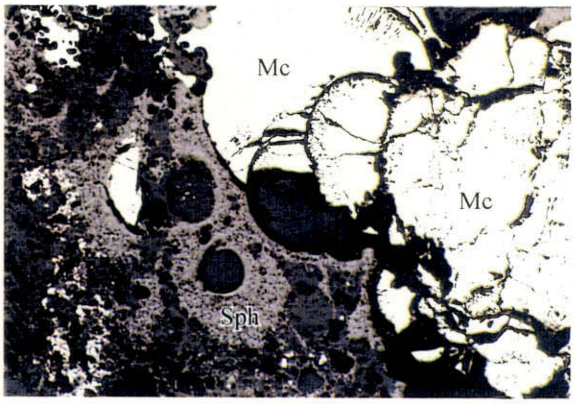

0 0.2 0.4mm

Drill-hole: **MJTK-L2** **Depth:** **277.00m** **Ore type:** **Veinlet**

The sample shows spherulite texture of ore minerals (several mm in diameter) in the matrix of quartz and other gangue minerals. Spherulites are composed of sphalerite, marcasite and gangue minerals. Some spherulites contain spherical material in its central part. The spherical materials are gangue minerals and are replaced completely or partly to marcasite or sphalerite, which form radial fine fabric aggregates. Other spherulites are composed of the aggregates of sphalerite showing framboidal texture. Sometimes the framboidal texture is elongated from center to rim of spherulite, and construct a radial texture as a whole. Dendritic marcasite grows radially on the spherical marcasite and framboidal sphalerite. The volume ratios of opaque minerals are 50 % for sphalerite, and 50 % for marcasite.

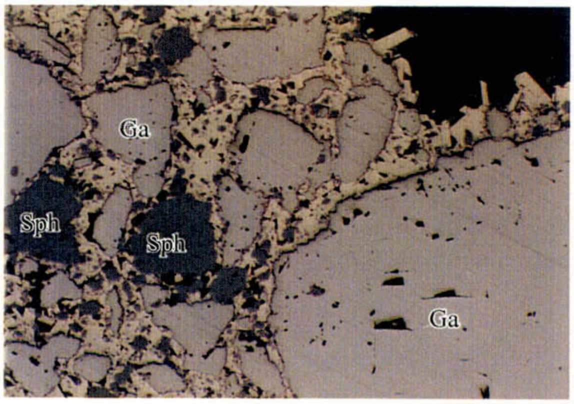

0 0.1 0.2mm

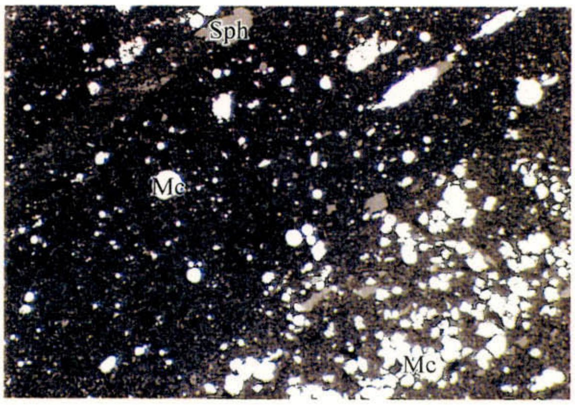

0 0.1 0.2mm

Drill-hole: **MJTK-L2** **Depth:** **297.60m** **Ore type:** **Banded**

The sample is composed of quartz band, galena-rich band and the band of framboidal pyrite. The galena-rich band is about 1 cm in thickness. The opaque minerals are galena (70 vol. %), sphalerite (20 %), marcasite (10%). Galena occurs as breccia like fragments up to 5 mm in size. The aggregates of anhedral sphalerite are also observed as similar fragments. These fragments are surrounded by subhedral sphalerite, euhedral marcasite and gangue minerals. Small amounts of framboidal pyrite and sphalerite occur in the band of framboidal pyrite. The size of the framboidal texture is from 0.2 to 0.5 mm in diameter.

Appendix 4 Microphotographs of ore polishes (2)

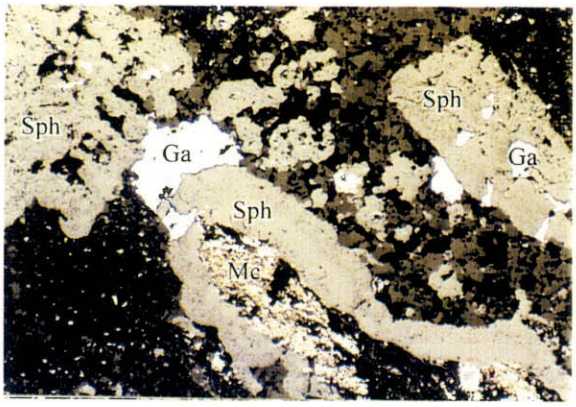

0 0.2 0.4mm

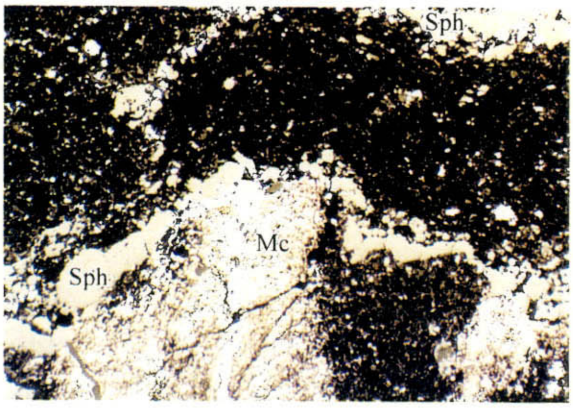

0 0.2 0.4mm

Drill-hole: **Depth:** **Ore type:**

MJTK-L2 298.60m Network Veins

The sample is network veins of sphalerite dominant ore. The polished section is composed of sphalerite (70 vol.%), marcasite (25%), galena (3 %) and pyrite (trace) as opaque minerals. Sphalerite occurs as anhedral to subhedral crystal up to 1 mm in diameter. Galena occurs as anhedral crystals up to 0.5 mm in size in the grain boundary of sphalerite crystals or inclusions in sphalerite. Marcasite occurs as an aggregate of euhedral grains up to 0.1 mm in size. Pyrite occurs as aggregates of very small subhedral grains up to 0.03 mm in size.

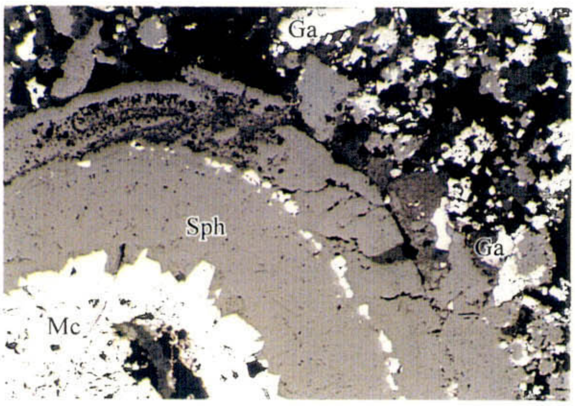

0 0.2 0.4mm

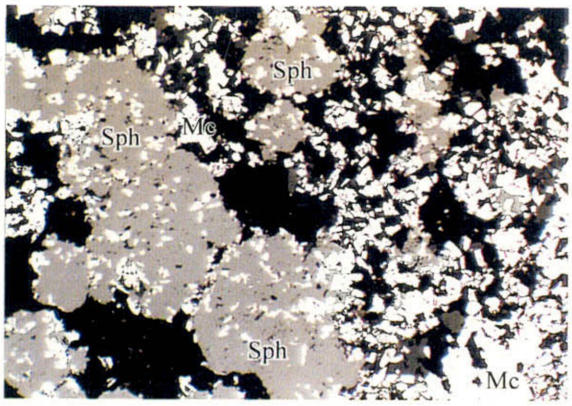

0 0.1 0.2mm

Drill-hole: **Depth:** **Ore type:**

MJTK-L2 299.60m Brecciated

The sample is a brecciated marcasite ore associated with some other minerals. Opaque minerals are consists of marcasite (70 vol.%) sphalerite (25 %) and galena (5 %). Marcasite occurs as euhedral grains with various sizes from 0.01 to 0.3 mm. The aggregates of marcasite show rhythmic or concentric banding by the difference of grain size. Sphalerite is precipitated during wide stage. The earlier sphalerite occurs as an oikocryst of poikilitic texture, containing marcasite as chadacryst. The later one overgrows on the marcasite, showing rhythmic banding. Galena occurs as anhedral crystals up to 1mm in diameter in the matrix of sphalerite and marcasite.

Appendix 4 Microphotographs of ore polishes (3)

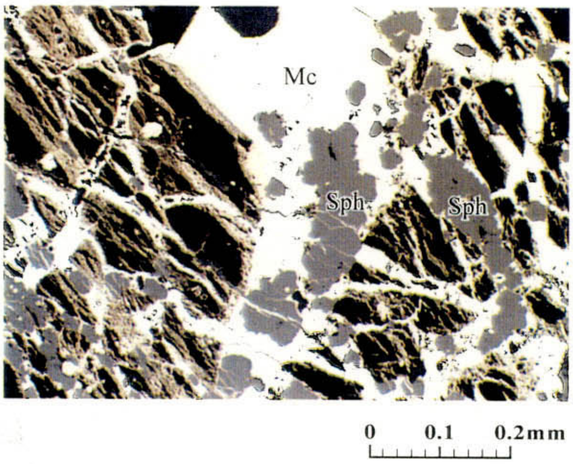

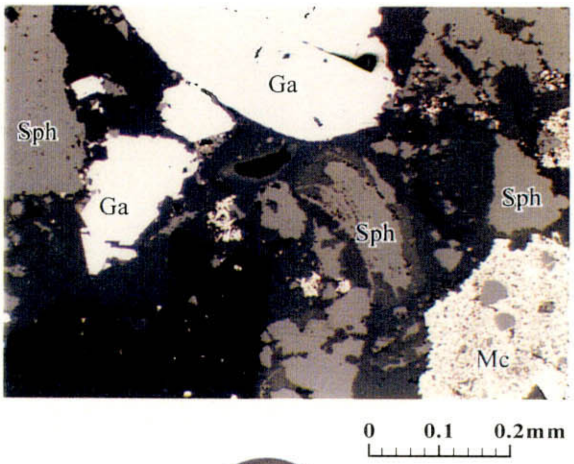

Drill-hole: **Depth:** **Ore type:**

MJTK-L2 300.60m Brecciated

The sample looks like conglomerate composed of angular fragments up to 7 mm in size. Some fragments are composed of angular galena, and others are composed of cracked sphalerite. Sphalerite occasionally contains many fine pyrite and marcasite to form disease texture. Broken piece of sphalerite with colloform texture, and aggregates of marcasite and sphalerite are also found as fragments. The matrix is composed mainly of quartz and carbonate. Small grains of marcasite are observed in the matrix. The contents are 50 vol.% for sphalerite, 30 % for galena, and 10 % for marcasite.

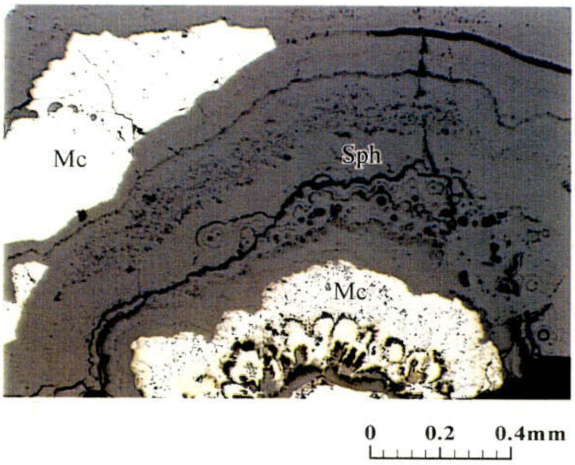

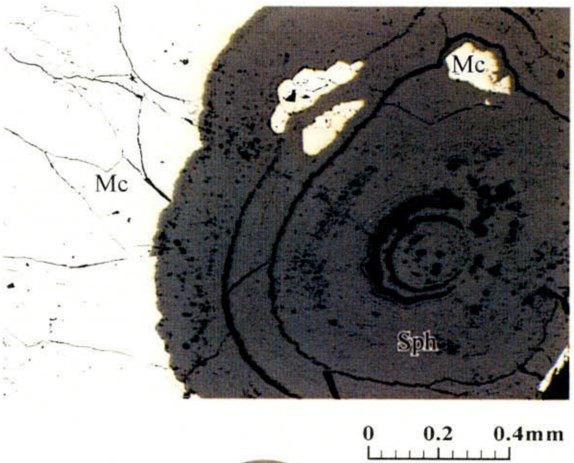

Drill-hole: **Depth:** **Ore type:**

MJTK-L2 301.60m Banded

The polished section is banded ore. Content of the band changes as follows in order of precipitation. That is, 1) mixture of marcasite and pyrite with galena, 2) dendritic goethite- sphalerite and pyrite which radiate in all directions, 3) mosaic marcasite of 0.1 mm in diameter, 4) sphalerite band with colloform texture, 4) large grains of marcasite up to 2 mm x 3 mm in size, and 5) sphalerite bands. The banding structure is prominent with iron content of sphalerite as well as existence of gangue minerals. Ordinal sphalerite is almost stoichiometric ZnS (Fe content is very low). Major minerals are sphalerite (65 %) and marcasite (30 %), and the others are minor minerals.

Appendix 4 Microphotographs of ore polishes (4)

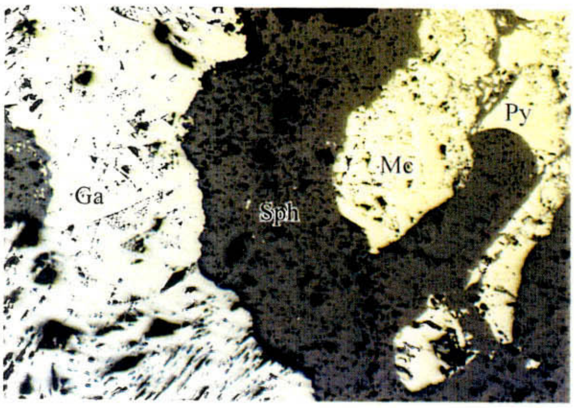

0 0.1 0.2mm

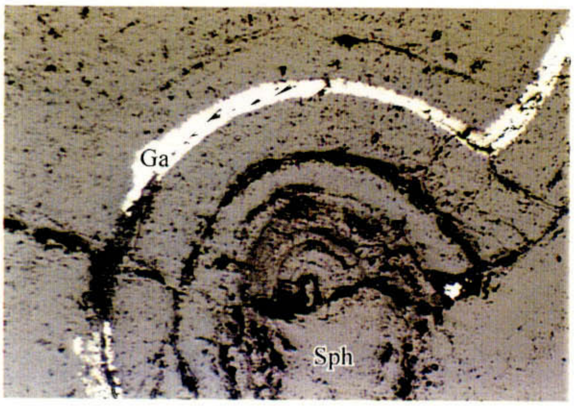

0 0.2 0.4mm

Drill-hole: **MJTK-L2** **Depth:** **380.60m** **Ore type:** **Brecciated**

The sample is a brecciated ore composed of galena (40 %), sphalerite (30 %), marcasite (20 %) and pyrite (10 %). Galena occurs as anhedral crystals up to 1mm in diameter, constructing the massive ore, which may be a part of vein. Small amount of galena occurs also as a thin layer (0.05 mm in width) in the concentric band of sphalerite. Pyrite occurs as euhedral grains up to 0.5 mm in size, and is surrounded by smaller grains of marcasite from 0.01 to 0.3 mm. Sphalerite is precipitated as aggregates, showing rhythmic banding.

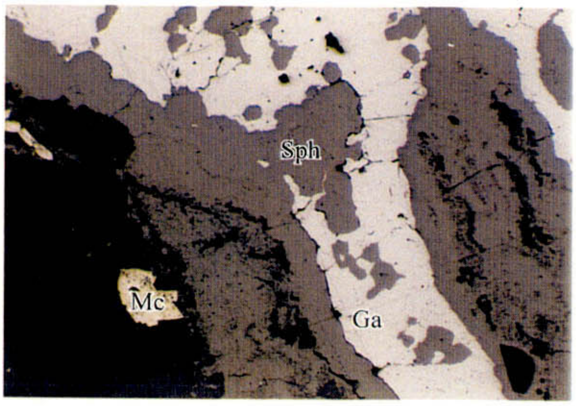

0 0.2 0.4mm

0 0.1 0.2mm

Koudiet Souda **Ore type:** **Veinlet**

The sample is veinlet of sphalerite (55 %) and galena (40 %) in the quartz-rich rock. The width of the veinlet varies from 0.1 to 5 mm. Sphalerite was precipitated with rhythmic banding texture at the earlier stage. At later stage, galena filled the central portion of the veinlet. The rock is also disseminated by pyrite (5 %).

Appendix 4 Microphotographs of ore polishes (5)

Appendix 5 Result of Chemical Analysis

No.	Drill Hole	Sampling Depth From	Sampling Depth To	Pb (ppm)	Zn (ppm)	Cu (ppm)	Cd (ppm)	Fe (%)	Mn (ppm)	$SrSO_4$ (%)	Ba (ppm)	Ca (%)	Mg (%)
1	MJTK-B1	47. 50	48. 50	38. 52	25. 36	55. 34	<2. 00	4. 23	829. 32	4. 83	148. 90	6. 70	2. 5
2	MJTK-B1	48. 50	49. 50	26. 96	<5. 00	39. 25	<2. 00	2. 91	512. 73	13. 50	229. 48	5. 30	1. 1
3	MJTK-B1	49. 50	50. 50	19. 47	38. 69	51. 81	<2. 00	4. 82	380. 39	20. 20	34. 55	1. 50	1. 0
4	MJTK-B1	50. 50	51. 50	23. 01	9. 87	91. 07	<2. 00	3. 38	779. 79	12. 70	16. 70	5. 40	1. 6
5	MJTK-B1	51. 50	52. 50	40. 95	271. 81	15. 38	<2. 00	4. 01	231. 15	25. 60	58. 69	1. 50	1. 0
6	MJTK-B1	52. 50	53. 50	49. 45	28. 70	67. 29	<2. 00	4. 34	145. 13	3. 50	163. 58	0. 30	0. 8
7	MJTK-B1	53. 50	54. 50	17. 27	195. 01	11. 96	<2. 00	2. 37	665. 44	23. 30	13. 20	3. 60	2. 1
8	MJTK-B1	54. 50	55. 50	27. 66	6. 07	30. 33	<2. 00	2. 91	410. 78	17. 40	95. 58	2. 50	1. 7
9	MJTK-B1	55. 50	56. 50	14. 36	<5. 00	23. 32	<2. 00	1. 44	26. 27	28. 20	135. 54	0. 10	0. 2
10	MJTK-B1	56. 50	57. 50	55. 16	<5. 00	9. 34	<2. 00	2. 85	177. 57	18. 40	125. 64	1. 20	0. 8
11	MJTK-B1	57. 50	58. 50	39. 47	78. 48	16. 72	<2. 00	2. 28	290. 11	18. 20	127. 38	1. 50	1. 2
12	MJTK-B1	59. 50	60. 50	48. 97	8. 49	24. 54	<2. 00	3. 92	490. 81	19. 20	95. 19	2. 00	1. 4
13	MJTK-B1	60. 50	61. 50	58. 27	127. 64	7. 80	<2. 00	6. 57	349. 48	21. 60	0. 95	1. 40	0. 6
14	MJTK-B1	61. 50	62. 50	49. 15	221. 56	16. 15	2. 47	7. 47	305. 40	25. 40	0. 33	1. 00	0. 7
15	MJTK-B1	62. 50	63. 50	51. 95	102. 52	15. 34	<2. 00	4. 54	122. 47	21. 80	61. 19	0. 18	0. 3
16	MJTK-B1	63. 50	64. 50	42. 42	<5. 00	14. 66	<2. 00	2. 47	324. 63	17. 50	155. 11	1. 80	1. 4
17	MJTK-B1	64. 50	65. 50	29. 76	531. 92	9. 30	<2. 00	2. 48	415. 85	16. 50	130. 90	2. 47	1. 7
18	MJTK-B1	67. 80	68. 80	41. 55	85. 77	8. 83	<2. 00	1. 68	1672. 73	8. 40	4. 64	14. 70	5. 9
19	MJTK-B1	68. 80	69. 80	68. 08	107. 11	25. 38	<2. 00	3. 56	849. 93	0. 13	338. 58	5. 70	3. 6
20	MJTK-B1	69. 80	70. 80	38. 18	368. 33	11. 65	<2. 00	2. 96	523. 15	8. 50	11. 85	4. 80	2. 8
21	MJTK-B1	70. 80	71. 80	60. 80	1844. 09	17. 03	<2. 00	4. 43	415. 06	9. 20	52. 75	2. 50	1. 7
22	MJTK-B1	71. 80	72. 80	55. 73	253. 95	23. 08	<2. 00	3. 43	843. 61	13. 90	11. 55	4. 40	2. 8
23	MJTK-B1	72. 80	73. 80	99. 50	72. 87	26. 14	<2. 00	5. 43	1308. 70	5. 30	2. 39	6. 90	4. 0

Appendix 5(Continued) Result of Chemical Analysis

No.	Drill Hole	Sampling Depth From	Sampling Depth To	Pb (ppm)	Zn (ppm)	Cu (ppm)	Cd (ppm)	Fe (%)	Mn (ppm)	Sr (ppm)	Ba (ppm)	Ca (%)	Mg (%)
24	MJTK-L1	102. 60	103. 60	81. 54	0. 15 (%)	0. 98	<2. 00	0. 31	159. 10	2972. 04	61. 07	16. 00	5. 25
25	MJTK-L1	103. 60	104. 60	23. 05	308. 24	8. 02	<2. 00	1. 18	175. 33	2798. 73	112. 04	10. 60	4. 35
26	MJTK-L1	104. 60	105. 60	<10. 00	76. 09	3. 71	<2. 00	0. 55	100. 10	2479. 18	100. 22	10. 00	2. 50

Appendix 5(Continued) Result of Chemical Analysis

No.	Drill Hole	Sampling Depth From	Sampling Depth To	Pb (ppm)	Zn (%)	Cu (ppm)	Cd (ppm)	Fe (%)	Mn (ppm)	Sr (ppm)	Ba (ppm)	Ca (%)	Mg (%)
27	MJTK-L2	222. 50	223. 50	186. 88	2. 00	6. 26	83. 58	1. 41	1318. 88	395. 09	11. 15	24. 20	6. 09
28	MJTK-L2	223. 50	224. 50	566. 50	1. 82	8. 93	73. 62	1. 59	1203. 45	435. 78	13. 58	20. 70	8. 00
29	MJTK-L2	224. 50	225. 50	330. 51	2. 45	12. 18	101. 41	2. 03	1441. 37	441. 05	30. 20	18. 70	8. 00
30	MJTK-L2	225. 50	226. 50	691. 19	2. 35	13. 95	88. 53	2. 43	1164. 89	820. 05	60. 47	24. 92	11. 93
31	MJTK-L2	226. 50	227. 50	1772. 08	4. 62	7. 02	189. 87	2. 55	1318. 41	518. 40	64. 47	35. 70	6. 79
32	MJTK-L2	227. 50	228. 50	1. 53 (%)	3. 52	1. 40	138. 27	2. 05	1277. 68	127. 51	7. 19	44. 10	3. 31
33	MJTK-L2	228. 50	229. 50	1053. 14	3. 07	7. 05	123. 95	1. 59	1583. 92	327. 98	25. 91	35. 00	13. 51
34	MJTK-L2	229. 50	230. 50	2451. 30	2. 82	6. 43	124. 51	0. 94	1191. 61	269. 83	37. 48	31. 22	12. 43
35	MJTK-L2	230. 50	231. 50	3252. 85	3. 70	11. 61	99. 13	2. 73	1160. 80	452. 00	151. 76	31. 60	9. 04
36	MJTK-L2	231. 50	232. 50	103. 70	1. 54	13. 55	56. 94	0. 93	764. 61	463. 16	31. 88	28. 00	14. 42
37	MJTK-L2	232. 50	233. 50	115. 78	3. 30	7. 38	161. 88	0. 98	912. 14	319. 35	30. 45	21. 60	8. 30
38	MJTK-L2	233. 50	234. 50	303. 57	2. 30	14. 32	41. 97	1. 22	1049. 71	570. 34	53. 39	21. 10	7. 30
39	MJTK-L2	234. 50	235. 50	137. 60	1. 40	7. 55	29. 19	1. 11	1054. 61	493. 57	13. 32	21. 20	8. 30
40	MJTK-L2	235. 50	236. 50	209. 03	1. 70	11. 52	16. 47	2. 09	1010. 61	633. 05	14. 51	20. 50	7. 00
41	MJTK-L2	236. 50	237. 50	103. 70	8. 42	9. 11	57. 17	5. 14	677. 82	511. 31	26. 28	35. 42	1. 32
42	MJTK-L2	237. 50	238. 50	6987. 99	20. 00	61. 79	132. 78	21. 00	372. 99	69. 09	113. 31	11. 62	0. 08
43	MJTK-L2	238. 50	239. 50	120. 34	0. 68	8. 82	9. 92	1. 22	644. 80	1257. 45	25. 22	44. 10	0. 33
44	MJTK-L2	265. 80	266. 80	776. 73	0. 81	11. 03	12. 08	2. 27	824. 54	489. 85	74. 70	22. 70	6. 70
45	MJTK-L2	266. 80	267. 80	516. 46	9. 46	22. 79	103. 08	2. 75	744. 12	346. 11	110. 96	32. 20	5. 33
46	MJTK-L2	267. 80	268. 80	518. 79	0. 79	13. 35	15. 48	3. 35	672. 39	825. 72	393. 59	38. 50	0. 91
47	MJTK-L2	268. 80	269. 80	874. 93	0. 69	11. 68	10. 90	4. 67	798. 02	693. 72	328. 33	37. 10	3. 81
48	MJTK-L2	269. 80	270. 80	5314. 89	1. 21	16. 64	32. 03	8. 55	560. 57	582. 88	394. 33	34. 62	0. 41
49	MJTK-L2	270. 80	271. 80	3064. 32	1. 03	19. 82	34. 03	5. 49	765. 72	432. 85	71. 91	39. 20	1. 40
50	MJTK-L2	271. 80	272. 60	1061. 45	0. 58	12. 51	15. 77	1. 39	822. 37	685. 65	338. 76	31. 08	13. 70
51	MJTK-L2	272. 60	273. 60	677. 67	1. 79	16. 67	43. 22	1. 30	889. 85	628. 58	85. 68	33. 04	11. 61
52	MJTK-L2	273. 60	274. 60	1871. 23	3. 47	28. 68	43. 14	3. 09	964. 97	805. 47	182. 12	33. 60	7. 21
53	MJTK-L2	274. 60	275. 60	5089. 43	3. 59	43. 85	61. 40	5. 53	822. 67	503. 13	113. 78	31. 22	6. 47
54	MJTK-L2	275. 60	276. 60	1. 92 (%)	36. 00	281. 47	506. 80	7. 50	292. 05	83. 07	7. 91	11. 20	0. 66
55	MJTK-L2	276. 60	277. 60	2621. 96	11. 30	50. 87	156. 67	6. 60	532. 78	523. 99	46. 70	33. 46	0. 16
56	MJTK-L2	277. 60	278. 60	144. 44	0. 59	14. 09	3. 92	1. 64	346. 56	991. 53	58. 65	39. 90	0. 25
57	MJTK-L2	291. 60	292. 60	1812. 00	1. 50	18. 00	14. 00	1. 05	612. 00	954. 00	225. 00	27. 14	0. 17

Appendix 5(Continued) Result of Chemical Analysis

No.	Drill Hole	Sampling Depth From	Sampling Depth To	Pb (ppm)	Zn (%)	Cu (ppm)	Cd (ppm)	Fe (%)	Mn (ppm)	Sr (ppm)	Ba (ppm)	Ca (%)	Mg (%)
58	MJTK-L2	292. 60	293. 60	2049. 25	0. 89	16. 32	20. 45	3. 46	560. 15	801. 16	109. 67	20. 90	0. 10
59	MJTK-L2	293. 60	294. 60	805. 22	0. 60	7. 86	16. 34	1. 54	529. 53	615. 29	107. 82	24. 10	0. 10
60	MJTK-L2	294. 60	295. 60	186. 59	1. 28	8. 90	23. 51	1. 50	712. 75	423. 64	270. 43	33. 00	0. 10
61	MJTK-L2	295. 60	296. 60	1090. 38	0. 59	12. 74	13. 93	2. 62	579. 94	799. 08	322. 84	30. 30	0. 10
62	MJTK-L2	300. 60	301. 60	132. 00	0. 54	9. 24	5. 29	1. 36	505. 63	903. 64	227. 46	31. 30	0. 20
63	MJTK-L2	301. 60	302. 60	131. 21	0. 51	10. 24	5. 11	1. 32	496. 02	877. 27	216. 74	30. 30	0. 20
64	MJTK-L2	302. 60	303. 60	327. 53	0. 31	7. 84	6. 32	1. 69	592. 69	494. 21	129. 99	31. 80	0. 30
65	MJTK-L2	303. 60	304. 60	418. 05	1. 65	19. 37	10. 17	3. 06	542. 20	732. 84	53. 01	26. 40	0. 90
66	MJTK-L2	345. 30	346. 30	433. 44	0. 39	17. 99	8. 13	1. 98	538. 87	1150. 60	162. 24	30. 80	0. 83
67	MJTK-L2	346. 30	347. 30	401. 40	1. 44	23. 33	11. 07	3. 83	502. 92	1631. 92	72. 94	23. 94	0. 25
68	MJTK-L2	347. 30	348. 30	3628. 01	4. 56	18. 34	37. 51	16. 00	431. 16	1181. 04	35. 96	21. 28	0. 16
69	MJTK-L2	348. 30	349. 30	1944. 27	8. 95	15. 59	58. 03	9. 40	348. 56	989. 65	55. 22	17. 92	0. 25
70	MJTK-L2	349. 30	350. 30	1537. 56	4. 01	6. 16	47. 21	4. 30	845. 58	840. 16	30. 20	40. 46	0. 16
71	MJTK-L2	350. 30	351. 30	2994. 26	0. 67	12. 88	6. 71	2. 41	855. 43	833. 31	163. 77	36. 40	0. 33
72	MJTK-L2	351. 30	352. 30	1291. 60	2. 21	16. 95	50. 11	3. 18	677. 18	1396. 61	211. 53	26. 04	0. 74
73	MJTK-L2	352. 30	353. 30	2735. 14	0. 63	22. 51	9. 09	3. 18	372. 61	1920. 87	167. 03	21. 98	0. 74
74	MJTK-L2	353. 30	354. 30	1. 74 (%)	1. 08	16. 80	52. 13	7. 12	429. 94	1573. 73	69. 51	20. 36	0. 83
75	MJTK-L2	354. 30	355. 30	1882. 06	0. 70	15. 71	4. 41	2. 30	600. 67	1771. 90	165. 90	33. 60	0. 74
76	MJTK-L2	355. 30	356. 30	1026. 53	1. 20	12. 39	14. 32	2. 43	697. 63	1291. 16	111. 30	39. 90	0. 41
77	MJTK-L2	356. 30	357. 30	2752. 52	2. 91	23. 70	41. 02	4. 36	417. 00	1867. 87	237. 95	22. 12	0. 75
78	MJTK-L2	357. 30	358. 30	662. 45	1. 13	17. 08	17. 01	4. 03	535. 15	1635. 15	104. 46	17. 08	3. 80
79	MJTK-L2	358. 30	359. 30	6637. 10	5. 94	26. 26	62. 10	7. 39	251. 14	1637. 83	72. 98	10. 92	0. 82
80	MJTK-L2	359. 30	360. 30	2818. 69	3. 37	26. 28	36. 96	3. 91	310. 51	1678. 22	108. 63	12. 32	0. 41
81	MJTK-L2	360. 30	361. 30	775. 14	1. 22	24. 43	12. 69	2. 96	248. 67	2025. 48	81. 34	10. 92	0. 33
82	MJTK-L2	361. 30	362. 30	6130. 81	3. 65	28. 35	40. 32	6. 37	196. 84	1523. 86	77. 07	7. 60	0. 41
83	MJTK-L2	362. 30	363. 30	945. 84	1. 61	26. 95	20. 22	4. 09	388. 53	1318. 75	244. 73	14. 84	0. 25
84	MJTK-L2	363. 30	364. 30	1190. 21	1. 72	35. 18	27. 89	4. 61	206. 34	1695. 02	173. 28	12. 32	0. 16
85	MJTK-L2	364. 30	365. 30	1216. 46	1. 42	60. 77	26. 89	4. 08	221. 42	2672. 97	117. 57	10. 08	0. 33
86	MJTK-L2	365. 30	366. 30	7677. 60	2. 30	76. 15	32. 15	3. 22	328. 42	3388. 34	69. 77	7. 20	0. 20
87	MJTK-L2	366. 30	367. 30	2342. 13	4. 30	45. 83	51. 53	2. 67	1204. 38	978. 18	111. 94	19. 90	0. 10
88	MJTK-L2	367. 30	368. 30	1. 92 (%)	1. 02	28. 84	70. 51	2. 65	963. 34	1124. 02	48. 99	17. 00	0. 20
89	MJTK-L2	368. 30	369. 30	1. 69 (%)	1. 06	39. 71	86. 35	2. 78	747. 59	934. 20	41. 92	14. 00	0. 20

Appendix 5(Continued) Result of Chemical Analysis

No.	Drill Hole	Sampling Depth From	Sampling Depth To	Pb (ppm)	Zn (ppm)	Cu (ppm)	Cd (ppm)	Fe (%)	Mn (ppm)	Sr (ppm)	Ba (ppm)	Ca (%)	Mg (%)
90	MJTK-L4	109.10	110.10	2338.20	371.92	8.63	2.63	1.09	1599.41	1268.81	>20000	31.00	0.30
91	MJTK-L4	110.10	111.10	6732.86	553.14	21.87	<2.00	1.72	1217.48	1397.73	>20000	22.80	0.86
92	MJTK-L4	111.10	112.10	379.27	216.28	22.77	<2.00	0.72	2221.72	2175.68	>20000	20.00	0.20
93	MJTK-L4	112.10	113.10	704.09	511.68	5.61	<2.00	0.69	1183.05	1797.08	>20000	19.20	0.22
94	MJTK-L4	113.10	113.70	1713.49	1656.80	8.42	5.14	0.91	1852.82	1917.04	>20000	27.50	0.29
95	MJTK-L4	173.20	174.20	446.30	2549.49	15.58	8.40	1.37	1339.14	891.64	>20000	30.00	0.56
96	MJTK-L4	174.20	175.20	1131.06	2776.17	14.97	6.50	1.53	907.63	780.75	>20000	29.00	1.00
97	MJTK-L4	175.20	176.20	734.91	1059.03	15.01	2.95	1.07	1212.83	1089.77	>20000	39.50	0.81
98	MJTK-L4	176.20	177.20	1349.40	1285.02	4.94	3.83	2.19	2702.88	785.64	>20000	39.00	1.28
99	MJTK-L4	177.20	178.20	455.15	1006.23	9.76	<2.00	0.98	792.14	718.40	>20000	35.00	0.69
100	MJTK-L4	178.20	179.20	174.54	1790.45	11.80	<2.00	0.94	960.78	1013.67	>20000	32.00	0.67
101	MJTK-L4	179.20	180.20	2105.44	3061.11	10.01	4.15	0.27	2377.77	590.17	>20000	31.00	2.15
102	MJTK-L4	180.20	181.20	662.13	2201.43	12.29	2.85	0.12	1246.32	745.62	>20000	33.00	0.64
103	MJTK-L4	181.20	182.20	1562.48	2500.99	13.63	<2.00	4.85	3213.37	995.25	>20000	28.90	2.70
104	MJTK-L4	182.20	183.20	9373.56	1184.03	19.98	2.76	3.59	2166.88	423.72	>20000	9.20	1.97
105	MJTK-L4	183.20	184.20	6838.91	1633.95	11.14	<2.00	4.64	2697.74	590.12	>20000	8.60	2.05
106	MJTK-L4	184.20	185.20	1.40 (%)	1380.89	26.13	6.72	3.85	2052.72	612.38	>20000	8.40	1.60
107	MJTK-L4	185.20	186.20	1.04 (%)	1381.48	66.75	2.06	6.25	3480.25	806.54	>20000	13.70	1.65
108	MJTK-L4	186.20	187.20	5807.00	1949.00	19.50	<2.00	0.39	2966.00	1125.00	>20000	18.00	3.50
109	MJTK-L4	187.20	188.20	736.03	1549.08	22.93	2.70	1.34	1182.47	1054.10	>20000	37.00	1.00